

# Self-Assembly of Tri-Pyrazolate Linked Cages with Di-Palladium Coordination Motifs

Xuan-Feng Jiang,<sup>a, b</sup> Wei Deng,<sup>b</sup> Rui Jin,<sup>b</sup> Lin Qin,<sup>b</sup> Shu-Yan Yu<sup>\*a, b</sup>

<sup>a</sup>Beijing Key Laboratory for Green Catalysis and Separation, Department of Chemistry and Chemical Industry, College of Environmental and Energy Engineering, Beijing University of Technology, Beijing 100124, P.R. China.

<sup>b</sup>Laboratory for Self-Assembly Chemistry, Department of Chemistry, Renmin University of China, Beijing 100872, China.

## Supporting Information

### Table of Contents

**S1.** Experimental Section

**S2.** Procedures

A. <sup>1</sup>H-NMR and mass spectrosopes of organic ligands H<sub>3</sub>L<sup>1</sup>~H<sub>3</sub>L<sup>5</sup>

B. <sup>1</sup>H-NMR and ESI (CSI)-MS spectral analysis of complexes **1~5**

**S3.** X-ray crystallography of complex **1-4**

**S4.** References

---

### **S1.** Experimental Section

All reactions and manipulations were carried out under an atmosphere of prepurified nitrogen using either Schlenk techniques. All the organic solvents were distilled from 4 Å molecular sieves under an argon atmosphere. The other chemical and all

commercially available reagents were used without any purification. NMR spectra of all compounds were recorded at 400 MHz on a Bruker AIVEN400 spectrometer. Halogenated and aromatic NMR solvents were dried over anhydrous potassium carbonate prior to use. The ESI-MS mass analyses were carried out by Bruker BIFLEX III spectrometer. The X-ray diffraction single-crystal data of complex **1-4** were collected on a Bruker Smart Apex CCD area detector equipped with a graphite monochromated MoK $\alpha$  radiation ( $\lambda = 0.71073 \text{ \AA}$ ).

**General tri(methylene)dipentane-2,4-dione Preparation (6 and 7).<sup>14-16</sup>**  
Acetylacetone (0.91 g, 0.91 mmol) was added during a 30-min period and stirred, refluxing solution prepared from potassium (350 mg, 0.9 mmol) and 40 ml of dried t-butyl alcohol. After 1 hours, the solution of tri(bromomethyl) compounds (3.1 mmol) in 20 ml of dried THF was added during a 30 min. After the addition, KI (10% quality of tri(bromomethyl) compounds) was added. The resultant solution was stirred and heated at reflux temperature (80 °C) until acidic to moist litmus (ca. 16 hours). After the solvent was distilled, the residue was washed with water and extracted with CH<sub>2</sub>Cl<sub>2</sub>. The organic phase was dried over anhydrous MgSO<sub>4</sub> and the solvent and excess acetylacetone was distilled. Further purification was achieved by recrystallization or by column chromatography, as noted below.

**1) Preparation of 1, 3, 5-tri((Z)-4-hydroxypent-3-en-2-one-3-yl)-methyl)-2, 4, 6-trimethyl benzene (6).**

Acetylacetone (4.50 g, 0.045 mol) was added during a 20-min period to a stirred, refluxing solution prepared from potassium (1.2 g, 0.03 mol) and 40ml of t-butyl

alcohol. After 50min, the solution of 1, 3, 5-tris(bromomethyl)-2, 4, 6-trimethyl benzene (3.7g, 0.01mol) in 50ml of THF was added during a 30 min. period and, 1 hr. after the addition, 0.3g of KI was added. The reaction mixture was stirred and heated at reflux temperature until acidic to moist litmus (ca. 24 hours). After three-fourths of the solvent was distilled, the residue was washed with water and extracted with benzene. The benzene extracts were dried over anhydrous  $Mg_2SO_4$  and the solvent and excess acetylacetone was distilled. Chromatography on silica gel elution with acetone/petroleum ether (1:4 v/v) afforded the intermediate **6** as light yellow oil. (1.4 g, 40%). Mp 150-156°C.  $^1H$  NMR (400 MHz,  $CDCl_3$ , 25°C, ppm):  $\delta$  3.85-3.81 (t,  $J$  = 7.4 Hz, 3H,  $\beta$ -diketone- $CH$ ), 3.25-3.23 (d,  $J$  = 7.4 Hz, 6H, Ar- $CH_2$ ), 2.19 (s, 9H, Ar- $CH_3$ ) 2.06 (s, 18H, Pz- $CH_3$ ).  $^{13}C$  NMR (100 MHz,  $CDCl_3$ , 25°C, ppm):  $\delta$  203.8, 134.2, 133.8, 67.3, 30.2, 29.1, 17.0. MS (EI) m/z: Anal. Calcd for  $[C_{41}H_{36}O_6+Na]^+$ , 479.24; Found: 479.24.

**2) Preparation of 1, 3, 5-tri((Z)-4-hydroxypent-3-en-2-one-3-yl)-methylphenyl-benzene (7).**

The above general tri( $\beta$ -diketone) preparation procedure was followed except for the substitution of 1,3,5-tris(bromomethyl)-2,4,6-triphenyl benzene (2.9 g, 5 mmol) in 100ml of t-butyl alcohol. Then the yellow solid **7** was obtained. (1.5 mg, 54%). Mp 163°C.  $^1H$  NMR (400 MHz,  $DMSO-d_6$ , 25°C, ppm):  $\delta$  7.74-7.28 (m, 12H, Ar-phenyl-H), 7.25 (d,  $J$  = 8.4 Hz, 6H, Ar-H), 4.06, 3.72, 3.21 (s, 6H, Ar- $CH_2$ -acac), 2.09 (s, 18H,  $CH_3$ -acac).  $^{13}C$  NMR (100 MHz,  $DMSO-d_6$ , 25°C, ppm):  $\delta$  203.1, 191.8,

142.4, 137.6, 129.5, 127.0, 125.34, 108.15, 69.7, 33.88, 30.83, 23.1, 21.07; MS (EI)

m/z: Anal. Calcd for  $[C_{42}H_{42}O_6+Na]^+$ , 665.39; Found: 665.28.

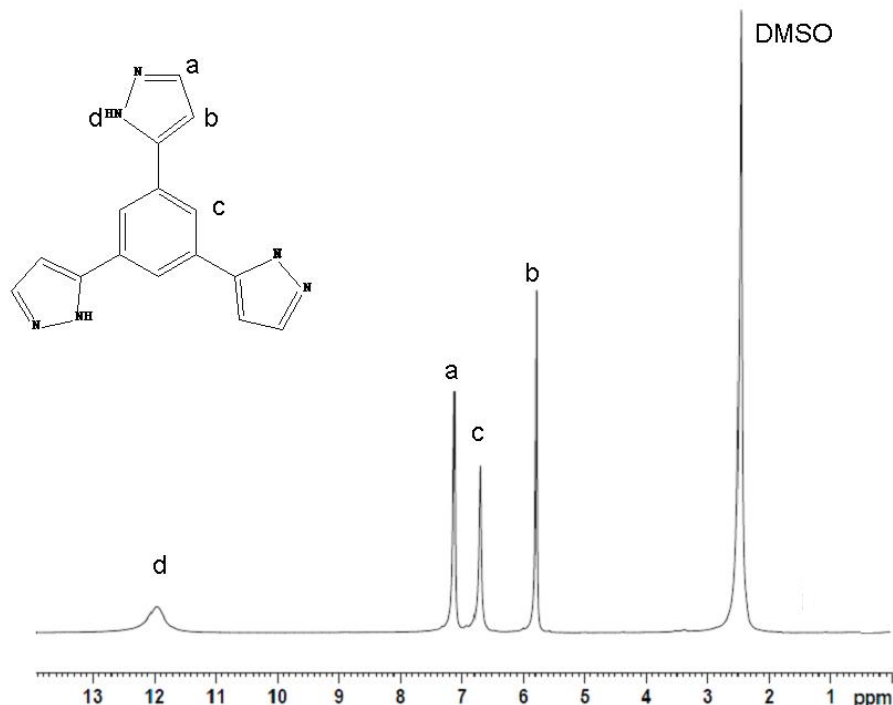


**Figure S1.** <sup>1</sup>H NMR spectrum of the 1, 3, 5 -tri(1*H*-pyrazol-3-yl)-benzene (**H<sub>3</sub>L<sup>1</sup>**) in DMSO-*d*6 at 298 K.

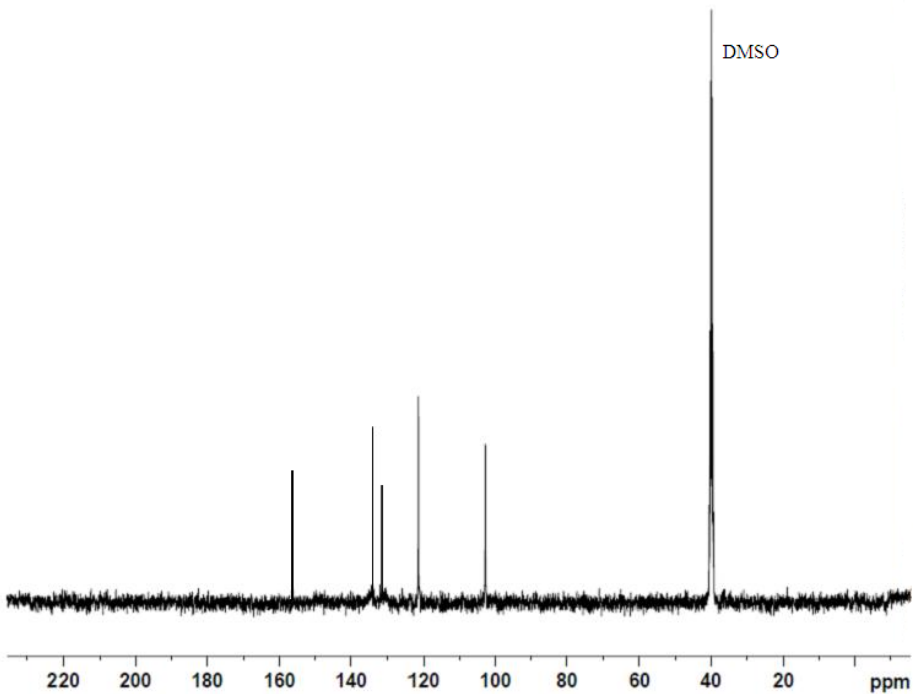


**Figure S2.** <sup>13</sup>C NMR spectrum of the 1, 3, 5 -tri(1*H*-pyrazol-3-yl)-benzene (**H<sub>3</sub>L<sup>1</sup>**) in DMSO-*d*6 at 298 K.

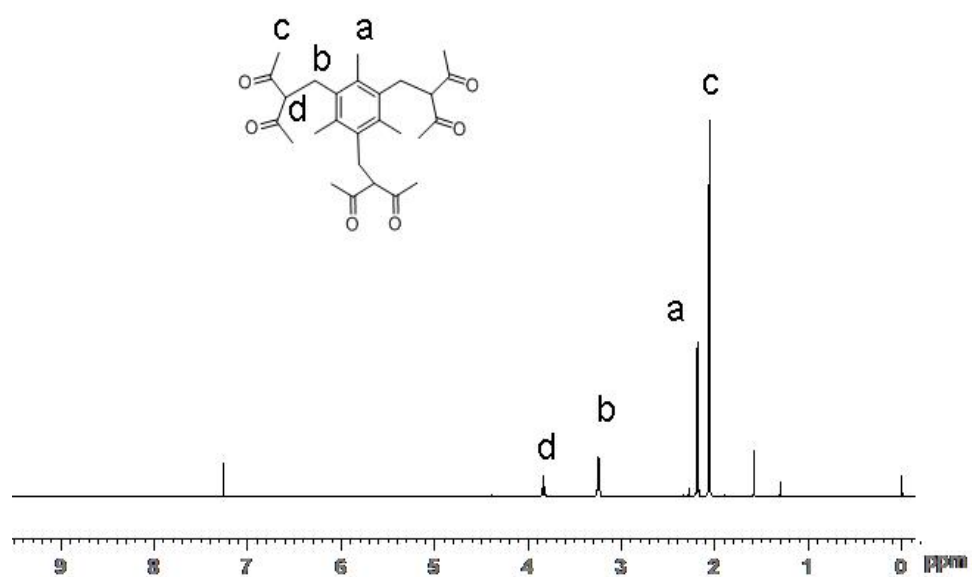


**Figure S3.** <sup>1</sup>H NMR spectrum of the 1, 3, 5-tri(((Z)-4-hydroxypent-3-en-2-one-3-yl)-methyl)-2,4,6-trimethyl benzene (**6**) in CDCl<sub>3</sub> at 298 K.

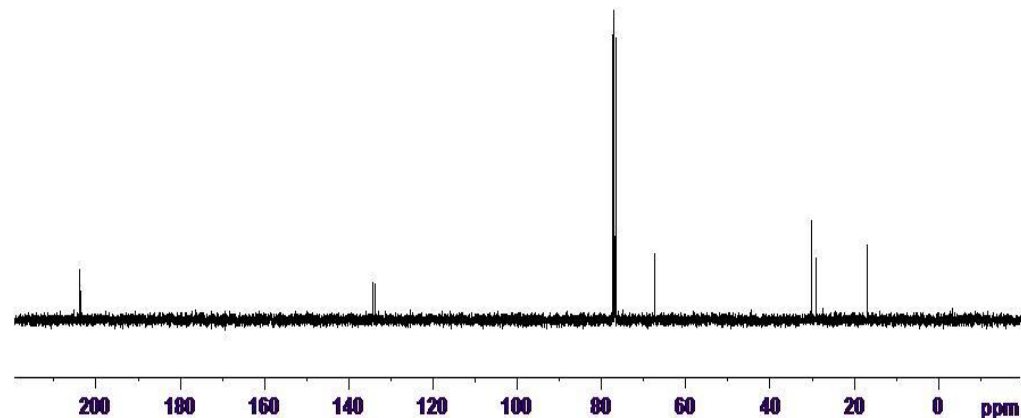


**Figure S4.** View of the <sup>13</sup>C NMR spectrum of the 1, 3, 5-tri(((Z)-4-hydroxypent-3-en-2-one-3-yl)-methyl)-2,4,6-trimethyl benzene (**6**) in CDCl<sub>3</sub> at 298 K.

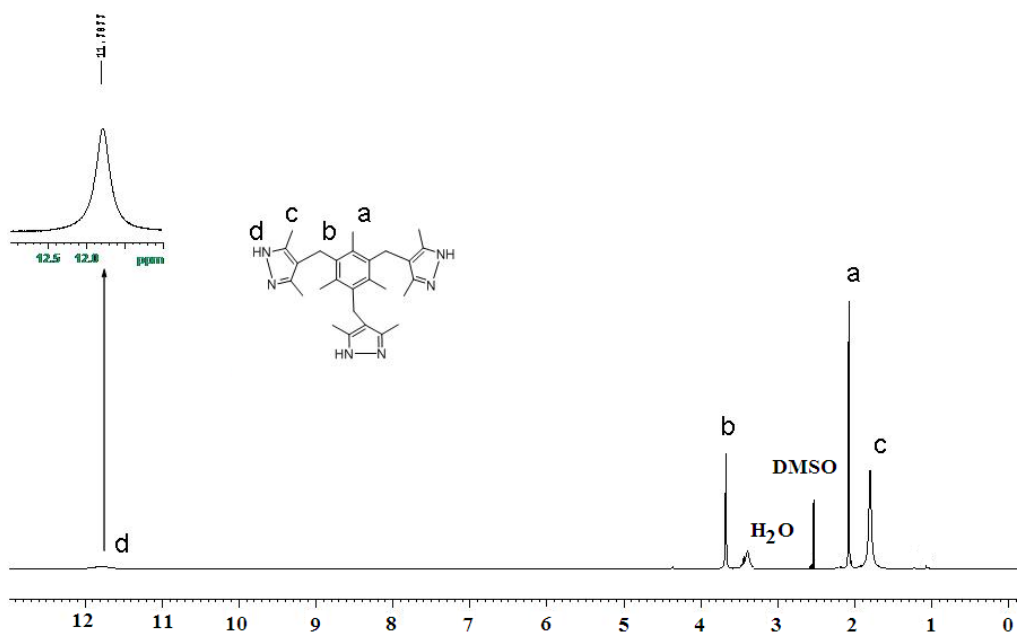


**Figure S5.** <sup>1</sup>H NMR spectrum of the 1, 3, 5 -tri((3, 5-dimethyl-1*H*-pyrazol-4-yl) methyl)-2,4,6-trimethyl benzene (**H<sub>3</sub>L<sup>4</sup>**) in DMSO-*d*6 at 298 K.

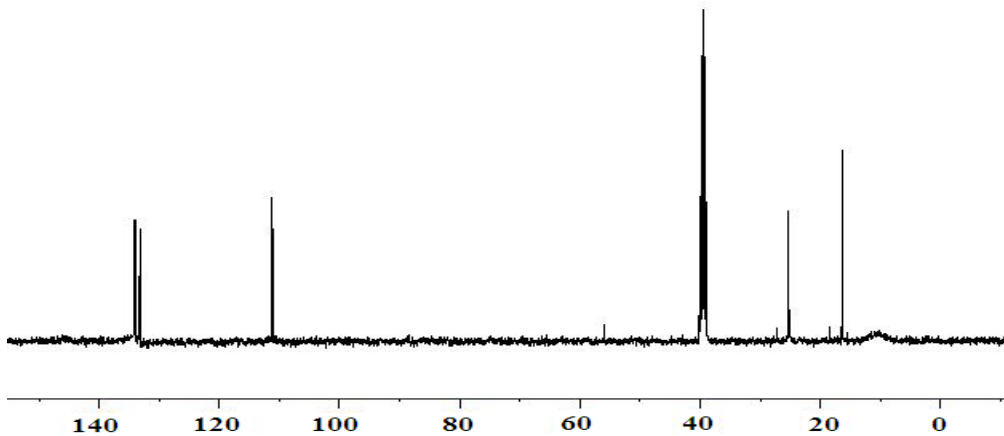


**Figure S6.** <sup>13</sup>C NMR spectrum of the 1, 3, 5 -tri((3, 5-dimethyl-1*H*-pyrazol-4-yl) methyl)-2,4,6-trimethyl benzene (**H<sub>3</sub>L<sup>4</sup>**) in DMSO-*d*6 at 298 K.

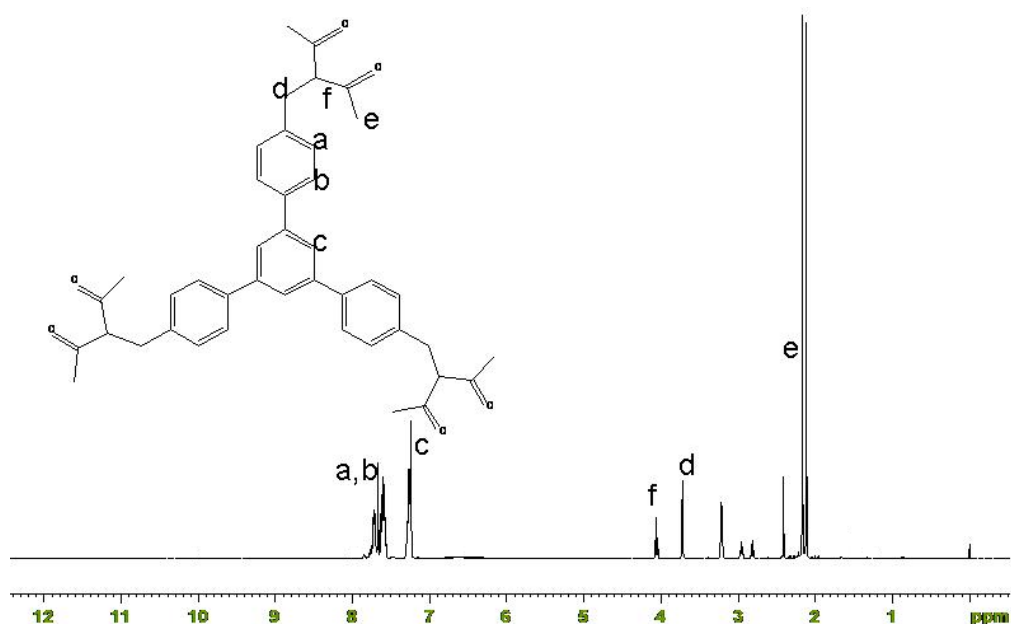


**Figure S7.**  $^1\text{H}$  NMR spectrum of the 1, 3, 5-tri(((Z)-4-hydroxypent-3-en-2-one-3-yl)-methylphenyl)-benzene in (7)  $\text{CDCl}_3$  at 298 K.

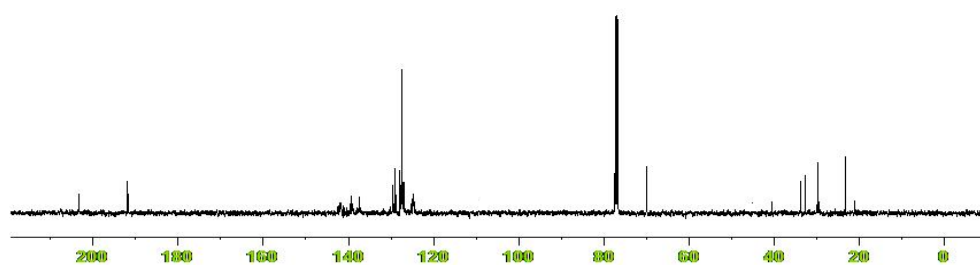


**Figure S8.**  $^{13}\text{C}$  NMR spectrum of the 1, 3, 5-tri((Z)-4-hydroxypent-3-en-2-one-3-yl)-methylphenyl)-benzene (**7**) in  $\text{CDCl}_3$  at 298 K.

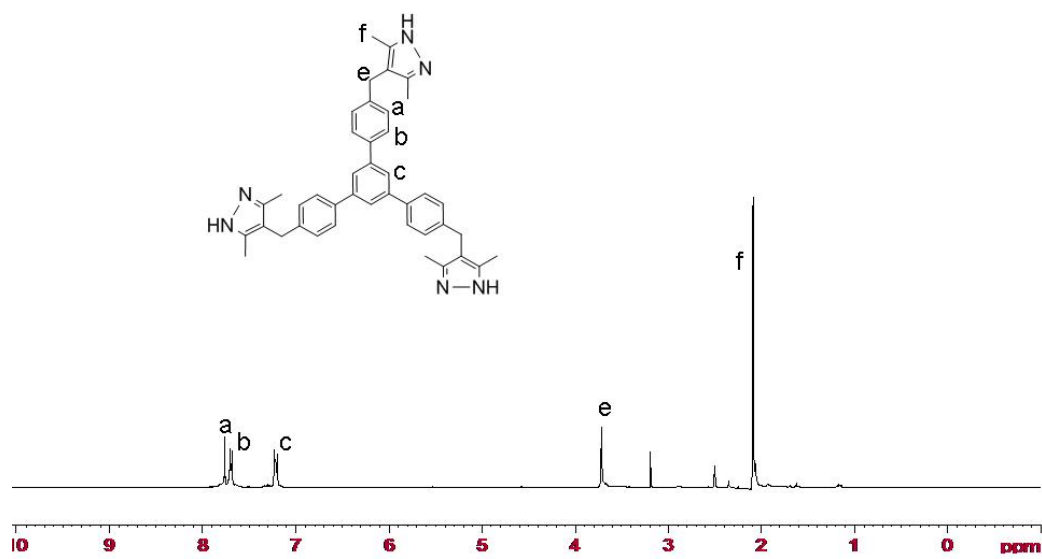


**Figure S9.** View of the  $^1\text{H}$  NMR spectrum of the 1, 3, 5-tri((3, 5-dimethyl-1*H*-pyrazol-4-yl)methyl)-phenyl)-benzene  $\mathbf{H}_3\mathbf{L}^5$  in  $\text{DMSO}-d_6$  at 298 K.

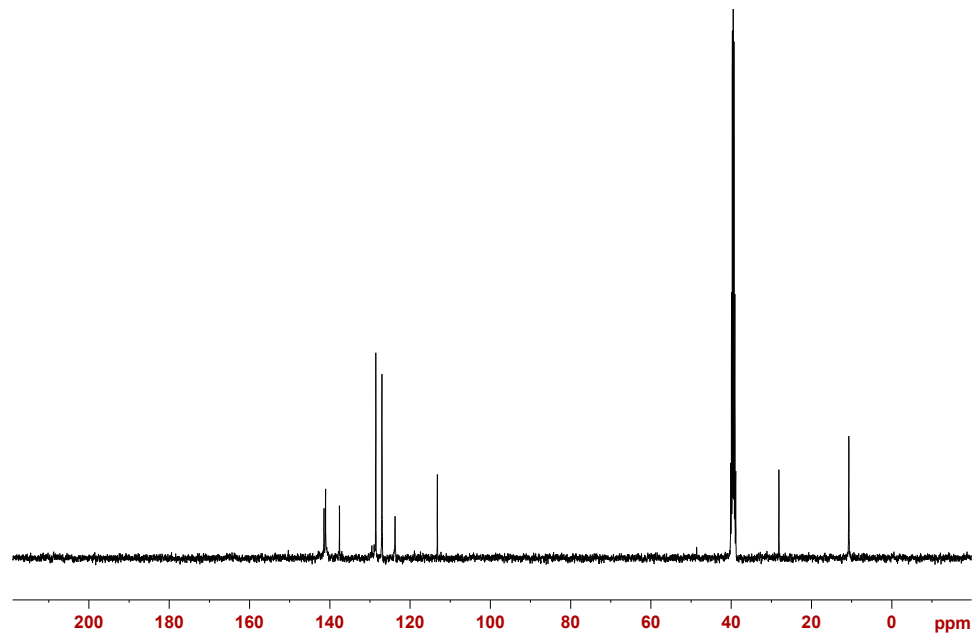


**Figure S10.** View of the  $^{13}\text{C}$  NMR spectrum of the 1, 3, 5-tri((3, 5-dimethyl-1*H*-pyrazol-4-yl)methyl)-phenyl)-benzene  $\mathbf{H}_3\mathbf{L}^5$  in  $\text{DMSO}-d_6$  at 298 K.

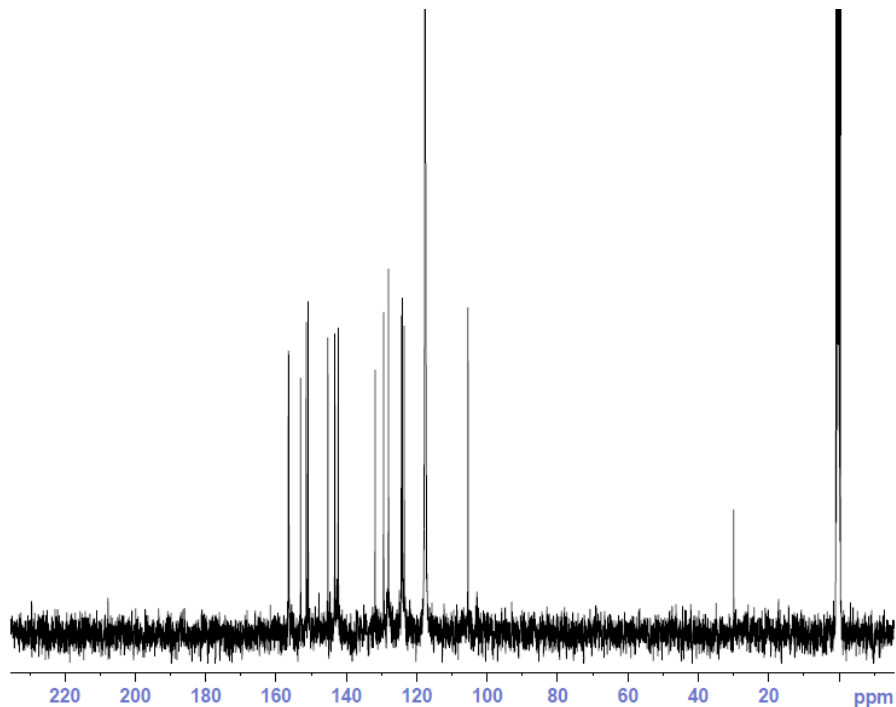


**Figure S11.**  $^{13}\text{C}$  NMR spectrum of  $\mathbf{1} \cdot 6\text{PF}_6$  in  $\text{CD}_3\text{CN}$  at 298 K.

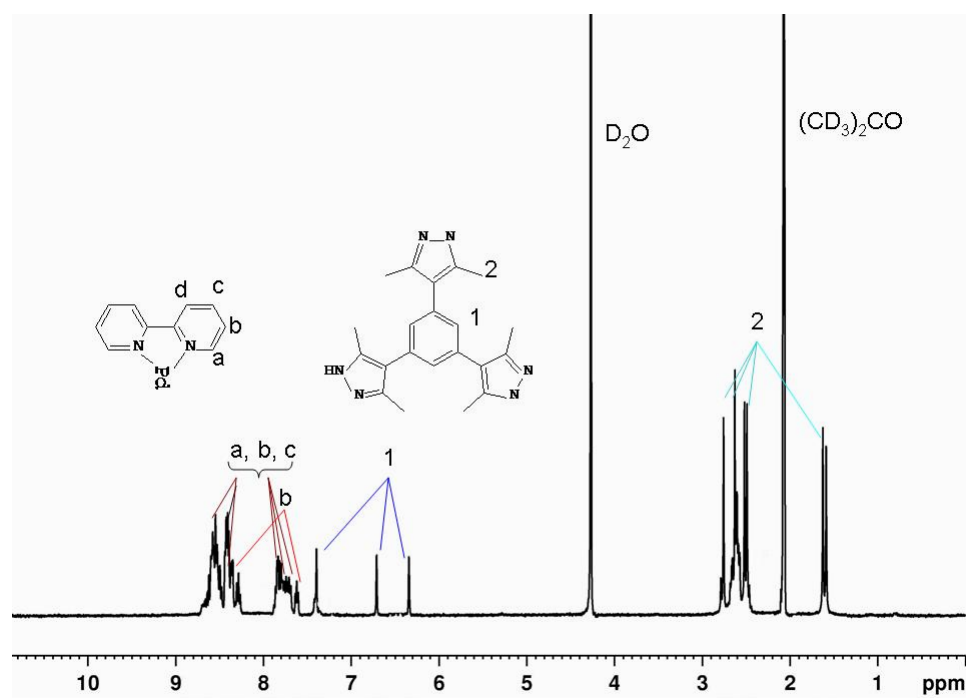


**Figure S12:** The  $^1\text{H}$  NMR spectrum of  $\mathbf{2a} \cdot 10\text{NO}_3^-$  in  $\text{CD}_3\text{CN}$  at 298 K.

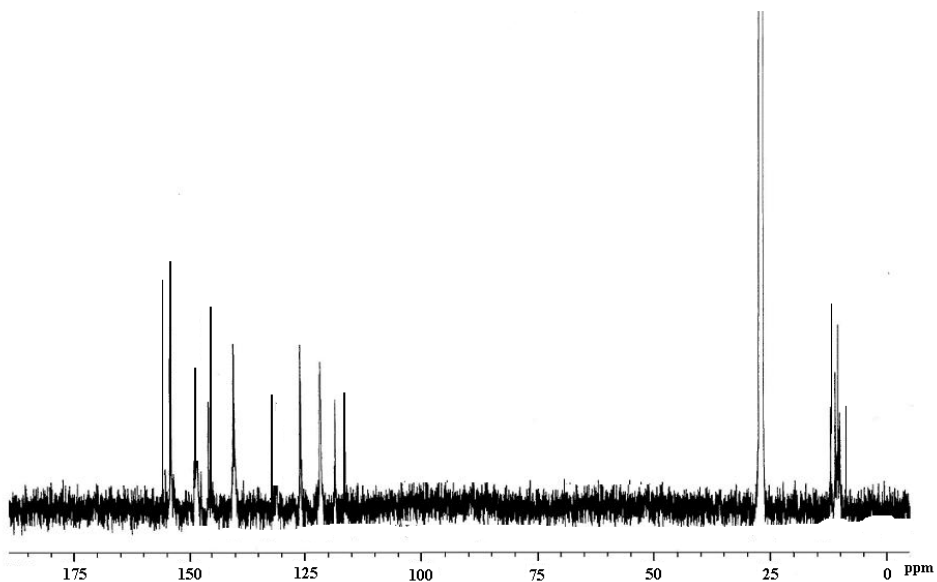


**Figure S13:** The  $^{13}\text{C}$  NMR spectrum of  $\mathbf{2a} \cdot 10\text{NO}_3^-$  in  $\text{CD}_3\text{CN}$  at 298 K.

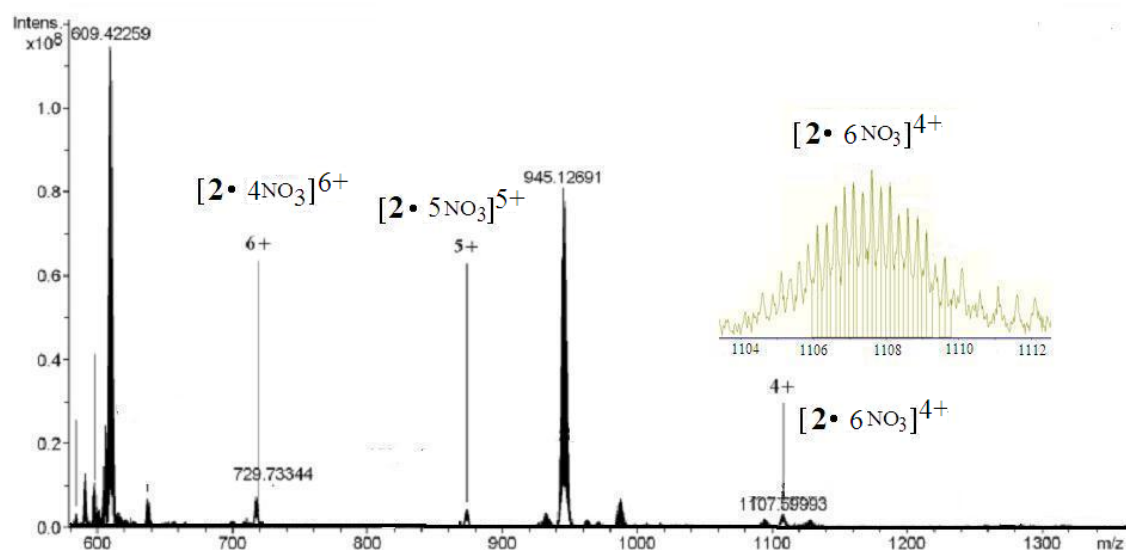


**Figure S14.** CSI-MS spectra of  $\mathbf{2a} \cdot 10\text{NO}_3^-$  in methanol; the inset shows the isotopic distribution of the species  $[\mathbf{2a} \cdot 6\text{NO}_3^-]^{4+}$ .

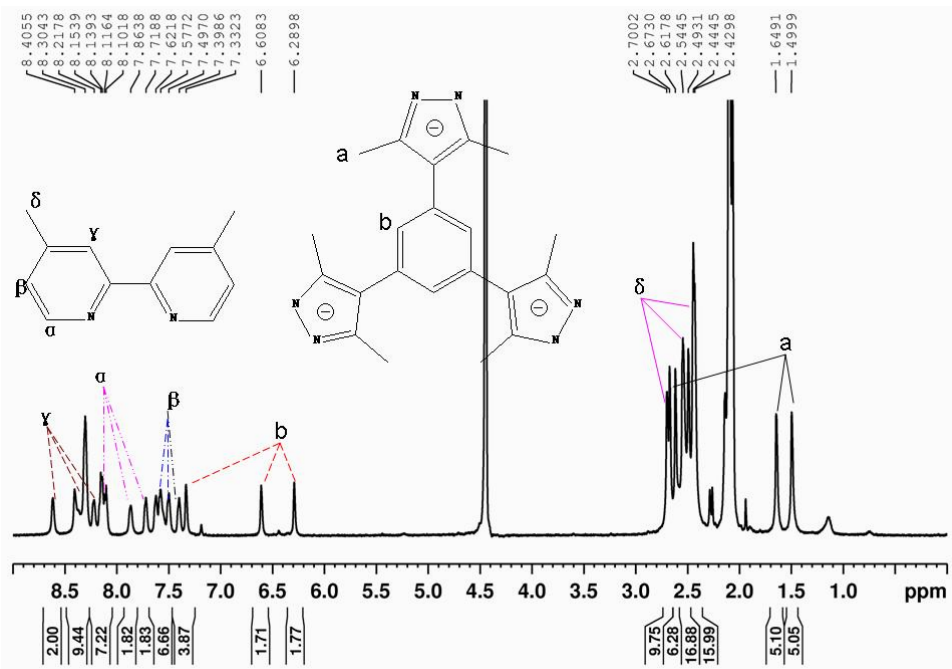


**Figure S15:** The  $^1\text{H}$  NMR spectrum of  $\mathbf{2b}\cdot 10\text{NO}_3^-$  in  $\text{CD}_3\text{COCD}_3/\text{H}_2\text{O}$  at 298 K.

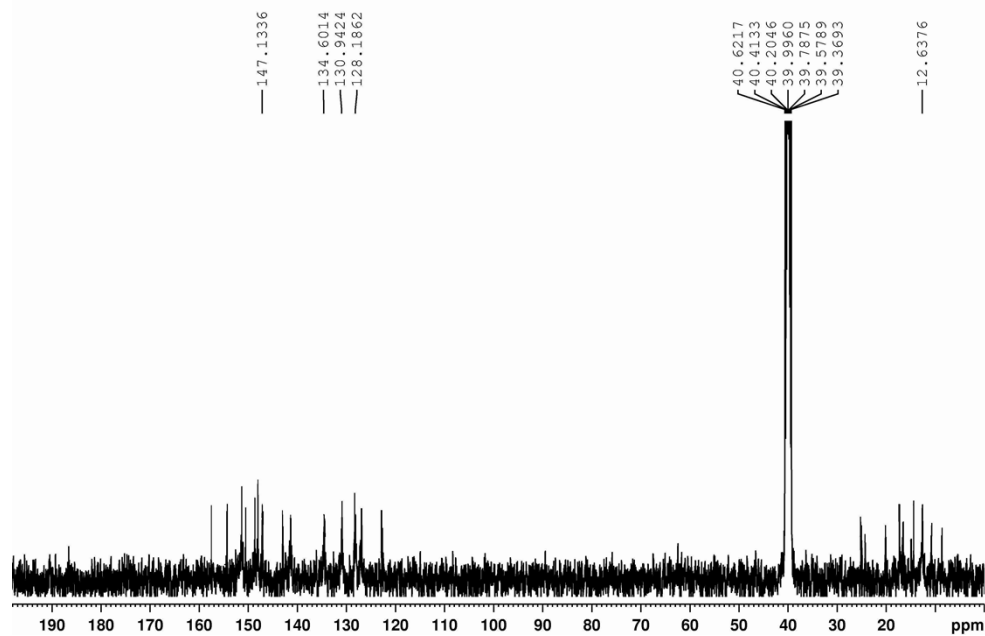


**Figure S16:** The  $^{13}\text{C}$  NMR spectrum of  $\mathbf{2b}\cdot 10\text{NO}_3^-$  in  $\text{DMSO-d}_6$  at 298 K.

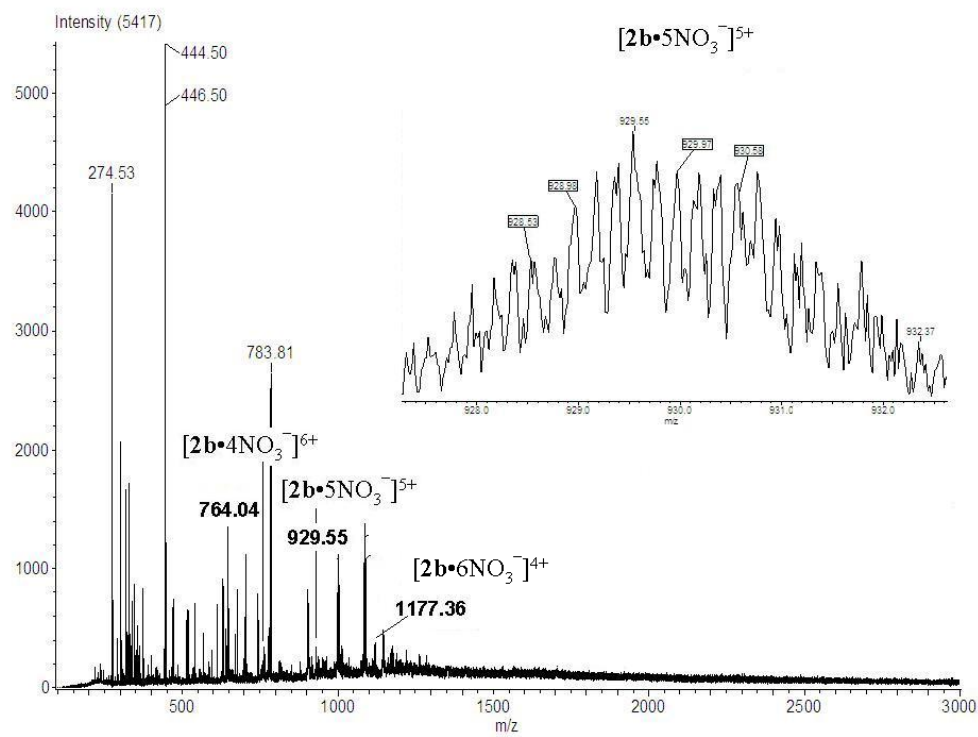


**Figure S17.** CSI-MS spectra of  $\mathbf{2b} \cdot 10\text{NO}_3^-$  in methanol; the inset shows the isotopic distribution of the species  $[\mathbf{2b} \cdot 5\text{NO}_3^-]^{5+}$ .

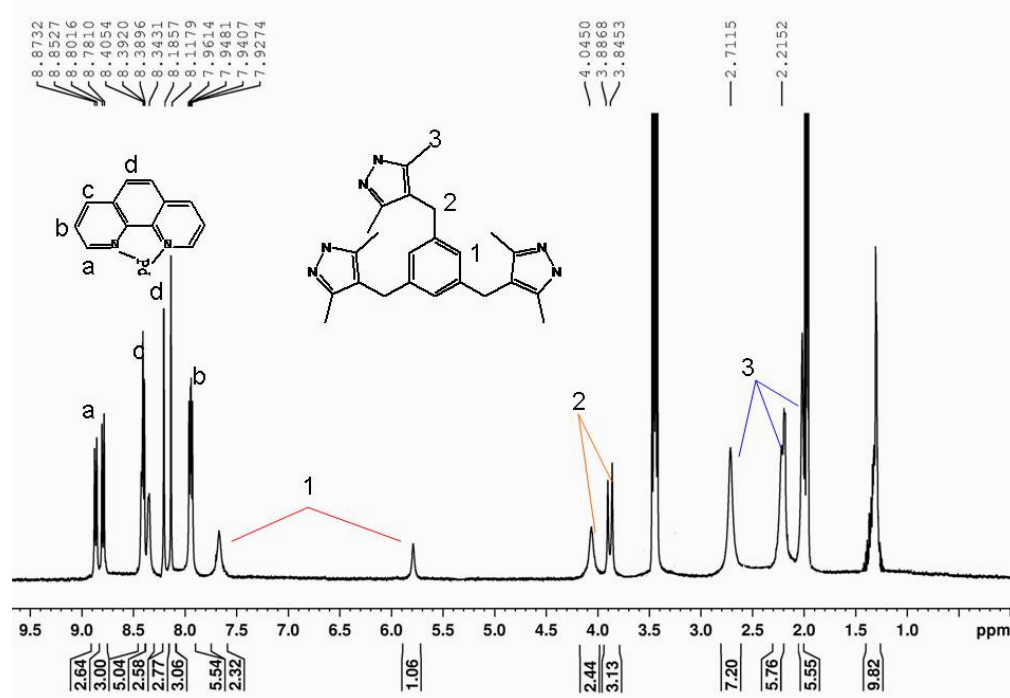


**Figure S18:** The  $^1\text{H}$  NMR spectrum of  $\mathbf{3} \cdot 12\text{NO}_3^-$  in  $\text{CD}_3\text{CN}$  at 298 K.

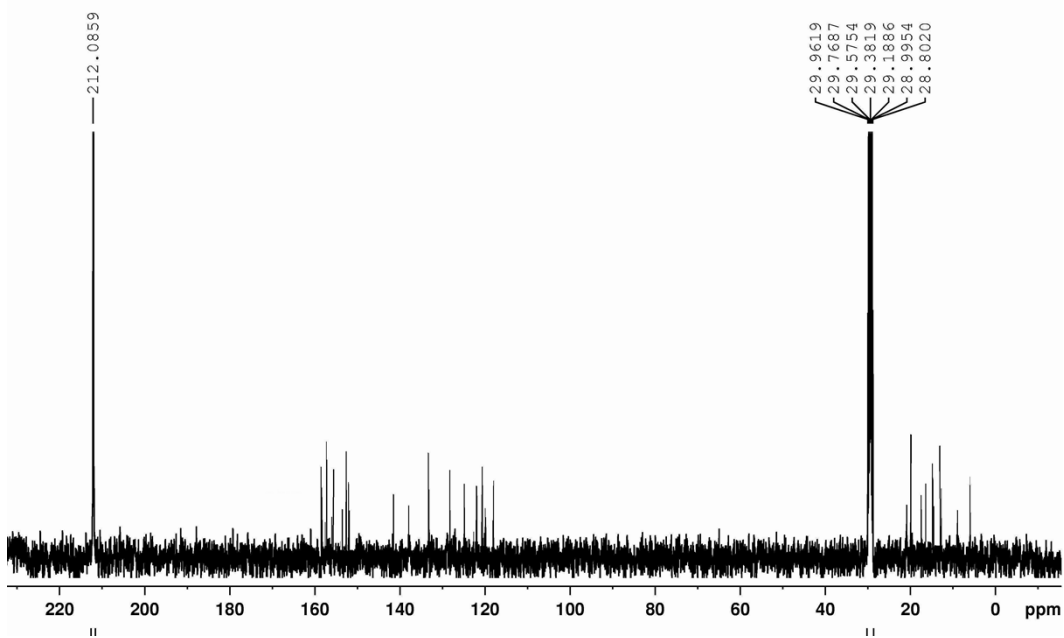


**Figure S19:** The  $^{13}\text{C}$  NMR spectrum of  $\mathbf{3} \bullet 12\text{NO}_3^-$  in  $\text{CD}_3\text{COCD}_3/\text{D}_2\text{O}$  at 298 K.

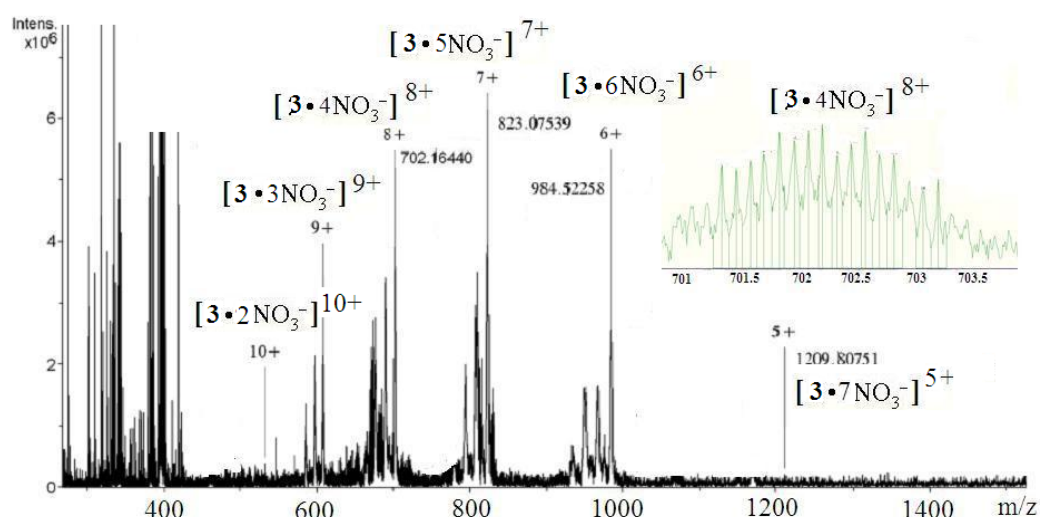


**Figure S20.** ESI-MS spectra of  $\mathbf{3} \bullet 12\text{PF}_6^-$  in methanol; the inset shows the isotopic distribution of the species  $[\mathbf{3} \bullet 4\text{PF}_6^-]^{8+}$ .

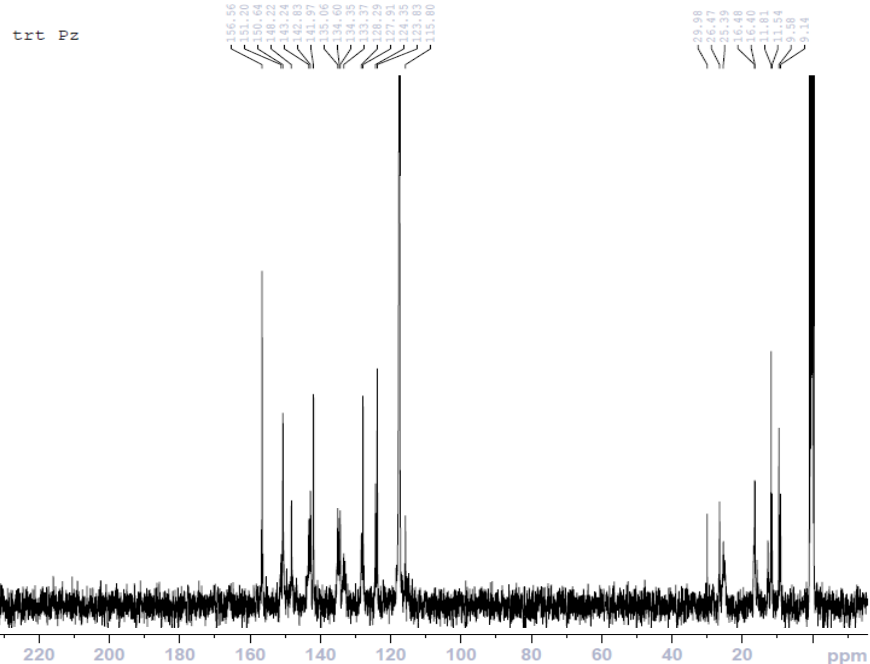


**Figure S21.** <sup>13</sup>C NMR spectrum of **4a** · 12PF<sub>6</sub> in CD<sub>3</sub>CN at 298 K.

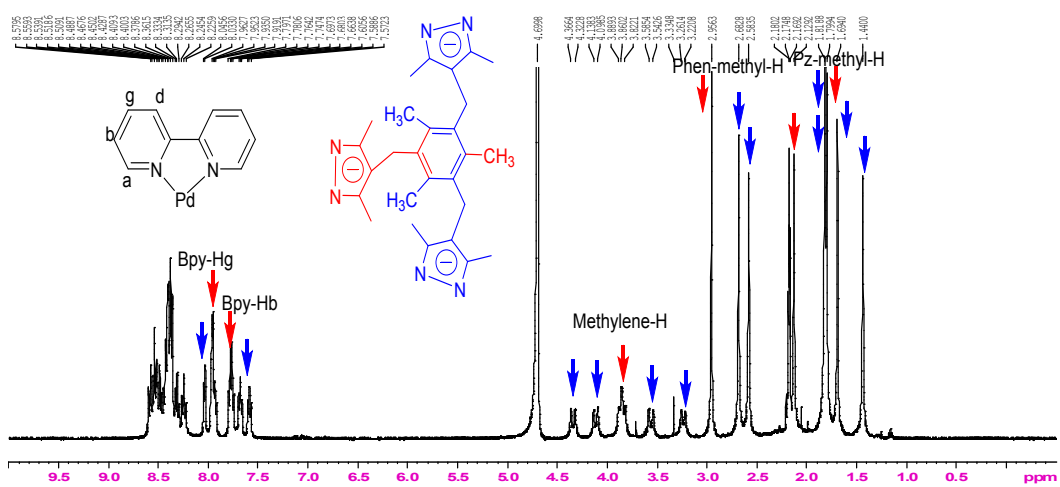


**Figure S22.** <sup>1</sup>H NMR spectra of complex **4a** · 12PF<sub>6</sub><sup>-</sup> (400 MHz, CD<sub>3</sub>CN, 25°C, TMS).

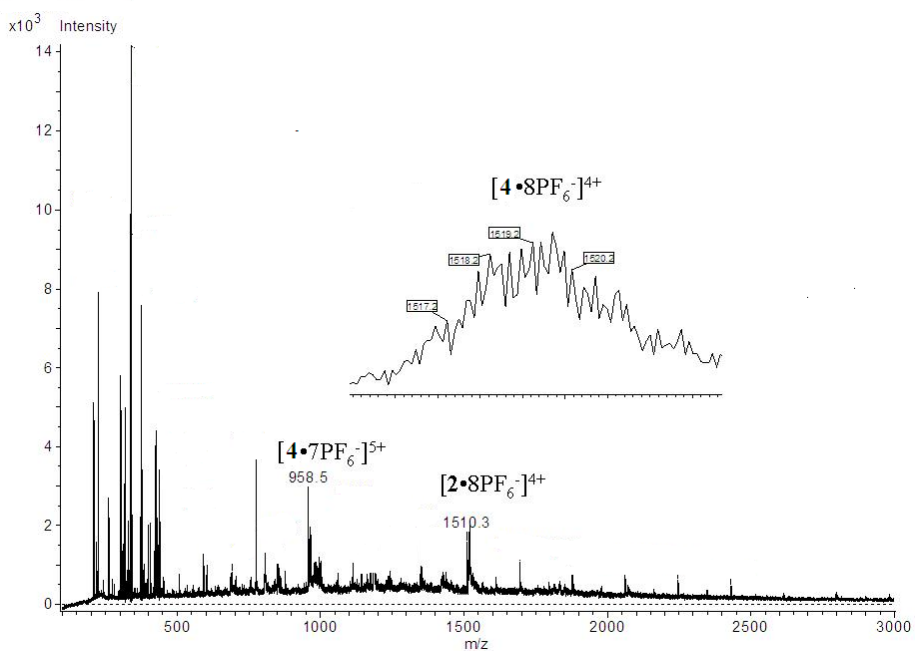


**Figure S23.** CSI-MS spectra of  $4\mathbf{a} \bullet 12\text{PF}_6^-$  in acetonitrile; the inset shows the isotopic distribution of the species  $[4\mathbf{a} \bullet 8\text{PF}_6^-]^{4+}$ .

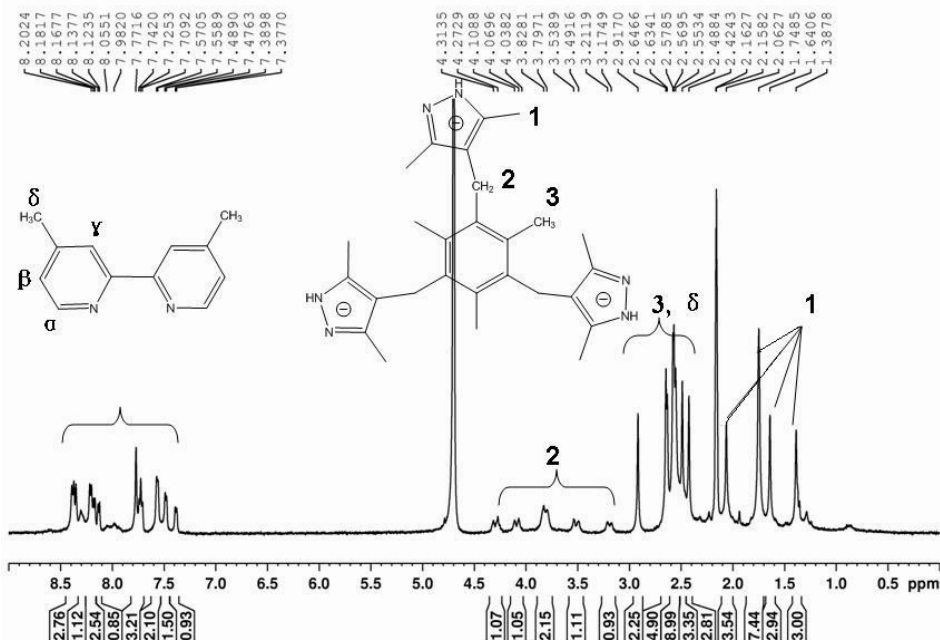


**Figure S24.**  $^1\text{H}$  NMR spectrum of  $4\mathbf{b} \bullet 10\text{NO}_3$  in  $\text{CD}_3\text{COCD}_3/\text{D}_2\text{O}$  at 298 K.

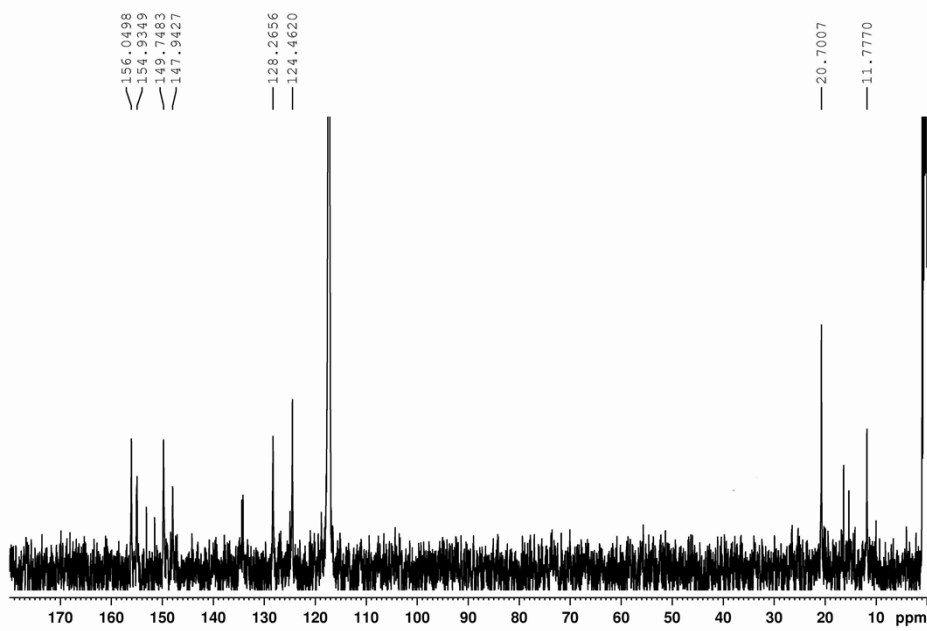


**Figure S25.**  $^{13}\text{C}$  NMR spectrum of  $\mathbf{4b} \bullet 10\text{PF}_6$  in  $\text{CD}_3\text{CN}$  at 298 K.

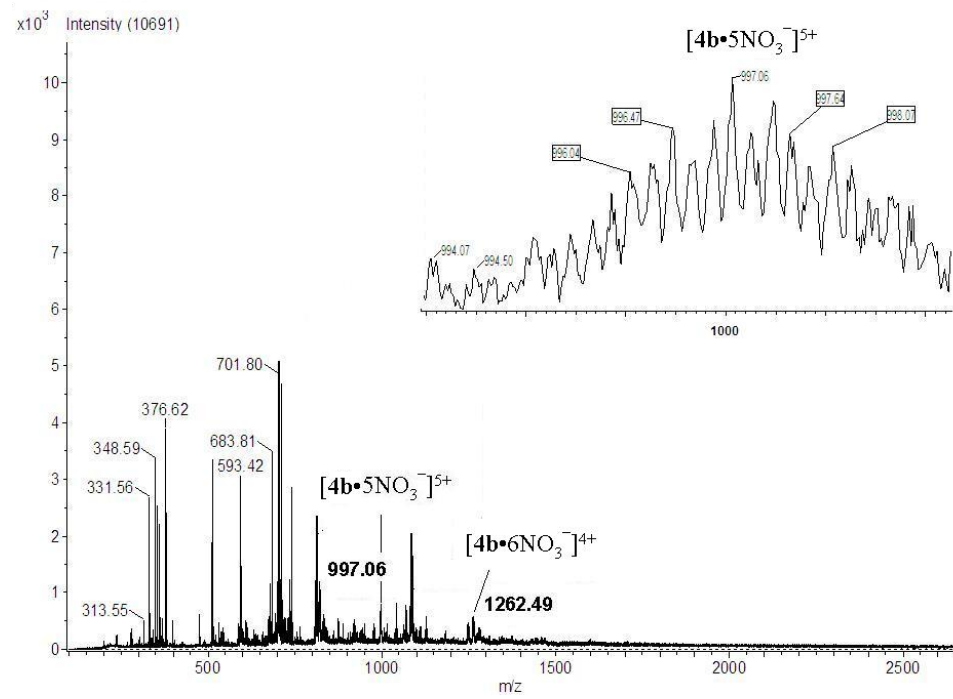


**Figure S26.** CSI-MS spectra of  $\mathbf{4b} \bullet 10\text{NO}_3^-$  in methanol; the inset shows the isotopic distribution of the species  $[\mathbf{4b} \bullet 5\text{NO}_3^-]^{5+}$ .

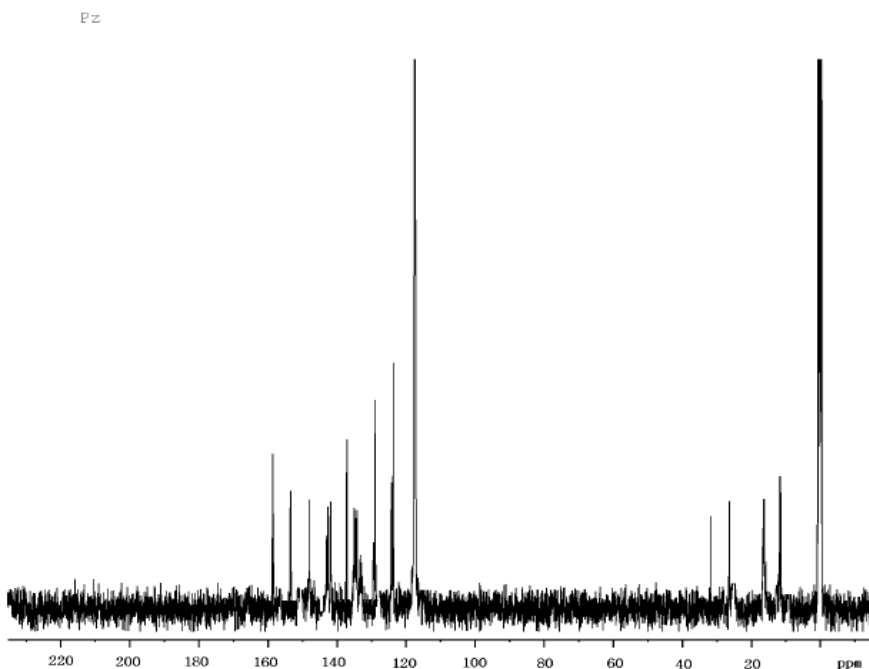


**Figure S27.** <sup>13</sup>C NMR spectrum of **5** · 6PF<sub>6</sub><sup>-</sup> in CD<sub>3</sub>CN at 298 K.

## S2. X-ray crystallography of complex **1** · 6NO<sub>3</sub><sup>-</sup>, **2** · 10NO<sub>3</sub><sup>-</sup>, **3** · 12PF<sub>6</sub><sup>-</sup> and **4b** · 10NO<sub>3</sub><sup>-</sup>

**X-ray Structural Determinations.** X-ray diffraction measurements were carried out at 291 K on a Bruker Smart Apex CCD area detector equipped with a graphite monochromated MoK $\alpha$  radiation ( $\lambda = 0.71073 \text{ \AA}$ ). The absorption correction for all complexes was performed using SADABS. All the structures were solved by direct methods and refined employing full-matrix least-squares on F2 by using SHELXTL (Bruker, 2000) program and expanded using Fourier techniques. All non-H atoms of the complexes were refined with anisotropic thermal parameters. The hydrogen atoms were included in idealized positions. In complex 1-3, the unit cell includes a large region of disordered solvent water molecules, which could not be modeled as discrete atomic sites. We employed PLATON/SQUEEZE to calculate the diffraction contribution of the solvent water molecules and, thereby, to produce a set of solvent-free H<sub>2</sub>O, CH<sub>3</sub>CN and anions diffraction intensities. Final residuals along with unit cell, space group, data collection, and refinement parameters are presented in Table S1-S6.

**Table S1.** Crystallographic data for complexes **1**, **2a**, **2b**, **3** and **4b**.

	<b>1</b> • 6NO <sub>3</sub>	<b>2a</b> • 10NO <sub>3</sub>	<b>2b</b> • 10NO <sub>3</sub>	<b>3</b> • 12PF <sub>6</sub>	<b>4b</b> • 10NO <sub>3</sub>
formula	C <sub>161</sub> H <sub>202</sub> N <sub>56</sub> O <sub>24</sub> Pd <sub>6</sub>	C <sub>184</sub> H <sub>188</sub> N <sub>52</sub> O <sub>36</sub> Pd <sub>10</sub>	C <sub>204</sub> H <sub>206</sub> N <sub>50</sub> O <sub>18</sub> Pd <sub>10</sub>	C <sub>240</sub> H <sub>204</sub> F <sub>72</sub> N <sub>48</sub> P <sub>12</sub> Pd <sub>12</sub>	C <sub>228</sub> H <sub>254</sub> N <sub>44</sub> Pd <sub>10</sub> •10(NO <sub>3</sub> )
FW	2122.07	4767.86	4710.20	6787.05	5294.85
crystal size [mm]	0.20×0.22×0.24	0.28×0.22× 0.20	0.10×0.10× 0.10	0.15×0.10× 0.10	0.10×0.10× 0.10
crystal system	Triclinic	Triclinic	Triclinic	Triclinic	Triclinic
space group	P-1	P-1	P-1	P -1	P-1
<i>a</i> [Å]	12.419(3)	16.367(9)	18.617(4)	21.424(4)	22.144(4)
<i>b</i> [Å]	16.935(3)	18.976(9)	19.665(4)	21.647(4)	25.555(5)
<i>c</i> [Å]	28.984(6)	21.069(11)	24.241(5)	23.509(5)	29.195(6)
<i>α</i> [°]	93.21(3)	94.611(12)	74.70(3)	67.45(3)	88.07(3)
<i>β</i> [°]	98.64(3)	107.429(14)	68.97(3)	68.36(3)	74.13(3)
<i>γ</i> [°]	108.50(3)	95.671(3)	84.45(3)	86.25(3)	71.95(3)
<i>V</i> [Å <sup>3</sup> ]	5680.14	6171(5)	7990(3)	9323(4)	15086(3)
Z	2	1	1	1	2
<i>ρ</i> <sub>calcd</sub> , [g/cm <sup>3</sup> ]	1.241	1.283	0.979	1.207	1.166
μ [mm <sup>-1</sup> ]	0.502	0.778	0.596	0.695	0.642
<i>F</i> (000)	3864	2404	2384.0	3360.0	5400.0
2θ <sub>max</sub> [°]	52.00	52.00	52.00	52.00	52.00
no. unique data	23204	24276	96542	45028	59243
parameters	1081	1408	1292	1731	2955
GOF [F <sup>2</sup> ] <sup>a</sup>	1.000	1.077	1.270	1.173	1.07
R [F <sup>2</sup> >2σ(F <sup>2</sup> )], wR[F <sup>2</sup> ] <sup>b</sup>	0.0545, 0.1264	0.0582, 0.1249	0.1114, 0.2960	0.0599, 0.1540	0.0519, 0.1545

[a] GOF =  $[w(F_o^2 - F_c^2)^2]/(n - p)^{1/2}$ , where  $n$  and  $p$  denote the number of data points and the number of parameters, respectively. [b] R1 =  $(|F_o| - |F_c|)/|F_o|$ ; wR2 =  $[w(F_o^2 - F_c^2)^2]/[w(F_o^2)^2]^{1/2}$ , Where  $w=1/[\sigma^2(F_o^2)+(aP)^2+bP]$  and  $P=[\max(0,F_o^2)+2F_c^2]/3$ .

**Table S2.** Selective bond distance ( $\text{\AA}$ ) and angle ( $^\circ$ ) of complex **1**•6NO<sub>3</sub><sup>-</sup>

Bond Dist.[ $\text{\AA}$ ]	Bond Dist.[ $\text{\AA}$ ]
N(1)-Pd(5)	1.984(6)
N(2)-Pd(5)	2.010(6)
N(3)-N(4)	1.388(9)
N(3)-Pd(5)	2.011(6)
N(4)-Pd(6)	2.027(6)
N(5)-Pd(6)	2.028(7)
N(6)-Pd(6)	2.010(7)
N(7)-N(8)	1.352(9)
N(7)-Pd(6)	2.006(7)
N(8)-Pd(5)	2.038(7)
N(9)-N(10)	1.346(8)
N(9)-Pd(4)	2.020(6)
N(10)-Pd(3)	2.022(6)
N(11)-Pd(3)	2.024(6)
N(12)-Pd(3)	2.020(6)
N(13)-N(14)	1.392(8)
N(13)-Pd(4)	2.007(7)
N(14)-Pd(3)	2.003(6)
N(15)-Pd(4)	1.991(6)
N(16)-Pd(4)	2.014(7)
N(17)-N(18)	1.371(8)
N(17)-Pd(2)	2.021(6)
N(18)-Pd(1)	2.001(6)
N(19)-Pd(2)	2.012(6)
N(20)-Pd(2)	2.022(6)
N(21)-N(22)	1.353(8)
N(21)-Pd(2)	2.032(6)
N(22)-Pd(1)	2.009(6)
N(23)-Pd(1)	2.021(6)
N(24)-Pd(1)	2.033(6)
N(25)-O(3)	1.190(13)
N(25)-O(1)	1.217(11)
N(25)-O(2)	1.230(13)
Pd(1)-Pd(2)	3.1185(11)
Pd(3)-Pd(4)	3.1731(12)
Pd(5)-Pd(6)	3.0701(1)
Bond Angel[ $^\circ$ ]	Bond Angel[ $^\circ$ ]
N(18)-Pd(1)-N(22)	82.4(2)
N(18)-Pd(1)-N(23)	97.9(2)
N(22)-Pd(1)-N(23)	177.3(2)
N(18)-Pd(1)-N(24)	176.2(2)
N(22)-Pd(1)-N(24)	98.8(3)
N(23)-Pd(1)-N(24)	80.8(2)
N(18)-Pd(1)-Pd(2)	64.87(15)
N(22)-Pd(1)-Pd(2)	65.33(16)
N(23)-Pd(1)-Pd(2)	112.39(16)
N(24)-Pd(1)-Pd(2)	112.25(17)
N(19)-Pd(2)-N(20)	81.6(2)
N(19)-Pd(2)-N(17)	94.2(2)
N(20)-Pd(2)-N(17)	175.8(2)
N(19)-Pd(2)-N(21)	176.8(2)
N(20)-Pd(2)-N(21)	95.5(2)
N(17)-Pd(2)-N(21)	88.8(2)
N(15)-Pd(4)-N(13)	176.4(3)
N(15)-Pd(4)-N(16)	80.6(3)
N(13)-Pd(4)-N(16)	95.9(3)
N(15)-Pd(4)-N(9)	95.8(3)
N(13)-Pd(4)-N(9)	87.8(3)
N(16)-Pd(4)-N(9)	176.2(3)
N(15)-Pd(4)-Pd(3)	119.24(18)
N(13)-Pd(4)-Pd(3)	61.86(18)
N(16)-Pd(4)-Pd(3)	120.86(18)
N(9)-Pd(4)-Pd(3)	61.66(16)
N(1)-Pd(5)-N(2)	81.4(3)
N(1)-Pd(5)-N(3)	95.4(3)
N(2)-Pd(5)-N(3)	176.8(3)
N(1)-Pd(5)-N(8)	178.4(3)
N(2)-Pd(5)-N(8)	97.3(3)
N(3)-Pd(5)-N(8)	85.9(3)

N(19)-Pd(2)-Pd(1)	117.99(17)	N(1)-Pd(5)-Pd(6)	115.23(19)
N(20)-Pd(2)-Pd(1)	119.18(16)	N(2)-Pd(5)-Pd(6)	117.17(19)
Pd(2)-Pd(1)	63.28(16)	N(3)-Pd(5)-Pd(6)	64.49(19)
Pd(2)-Pd(1)	62.57(17)	N(8)-Pd(5)-Pd(6)	64.5(2)
N(14)-Pd(3)-N(12)	174.6(3)	N(7)-Pd(6)-N(6)	98.3(3)
N(14)-Pd(3)-N(10)	83.3(3)	N(7)-Pd(6)-N(4)	83.8(3)
N(12)-Pd(3)-N(10)	98.0(3)	N(6)-Pd(6)-N(4)	177.3(3)
N(14)-Pd(3)-N(11)	97.8(3)	N(7)-Pd(6)-N(5)	178.2(2)
N(12)-Pd(3)-N(11)	80.3(3)	N(6)-Pd(6)-N(5)	80.0(3)
N(10)-Pd(3)-N(11)	173.5(2)	N(4)-Pd(6)-N(5)	97.9(3)
N(14)-Pd(3)-Pd(4)	65.06(17)	N(7)-Pd(6)-Pd(5)	65.01(18)
N(12)-Pd(3)-Pd(4)	110.80(17)	N(6)-Pd(6)-Pd(5)	113.0(2)
N(10)-Pd(3)-Pd(4)	64.34(17)	N(4)-Pd(6)-Pd(5)	66.25(18)
N(11)-Pd(3)-Pd(4)	110.26(17)	N(5)-Pd(6)-Pd(5)	115.06(19)

**Table S3.** Selective bond distance (Å) and angle (°) of complex **2a**•10NO<sub>3</sub><sup>-</sup>

Bond Dist.[Å]		Bond Dist.[Å]	
N(1)-N(2)	1.378(6)	N(14)-Pd(1)	2.005(4)
N(1)-Pd(1)	2.008(4)	N(15)-Pd(2)	2.029(4)
N(3)-N(4)	1.365(5)	N(16)-Pd(2)	2.028(4)
N(3)-Pd(2)	2.035(4)	N(17)-Pd(3)	2.019(4)
N(4)-Pd(3)	2.010(4)	N(18)-Pd(3)	2.026(4)
N(5)-N(6)	1.351(6)	N(19)-Pd(4)	2.028(4)
N(5)-Pd(4)	2.032(4)	N(20)-Pd(4)	2.030(4)
N(6)-Pd(5)	2.007(4)	N(21)-Pd(5)	2.017(4)
N(7)-N(8)	1.361(6)	N(22)-Pd(5)	2.019(4)
N(8)-Pd(1)#1	2.025(4)	Pd(1)-N(8)#1	2.025(4)
N(9)-N(10)	1.355(6)	Pd(2)-Pd(3)	3.1276(12)
N(9)-Pd(2)	2.020(4)	Pd(4)-Pd(5)	3.2361(12)
N(10)-Pd(3)	2.014(4)	N(11)-N(12)	1.357(5)
N(12)-Pd(5)	2.030(4)	N(11)-Pd(4)	2.000(4)
N(13)-Pd(1)	2.033(4)		

Bond	Angel[°]	Bond	Angel[°]
N(2)-N(1)-Pd(1)	120.0(3)	C(29)-N(7)-N(8)	109.8(4)
N(1)-N(2)-C(10)	111.0(3)	N(7)-N(8)-C(31)	108.0(3)
C(13)-N(3)-N(4)	110.9(3)	N(7)-N(8)-Pd(1)#1	119.4(3)
C(13)-N(3)-Pd(2)	132.7(3)	C(31)-N(8)-Pd(1)#1	127.3(3)
N(4)-N(3)-Pd(2)	112.7(3)	C(34)-N(9)-N(10)	109.6(3)
C(15)-N(4)-N(3)	107.0(3)	C(34)-N(9)-Pd(2)	130.0(3)
C(15)-N(4)-Pd(3)	128.7(2)	N(10)-N(9)-Pd(2)	115.0(3)
N(3)-N(4)-Pd(3)	119.0(3)	C(36)-N(10)-N(9)	108.9(3)
N(6)-N(5)-C(18)	110.7(3)	C(36)-N(10)-Pd(3)	130.4(3)
N(6)-N(5)-Pd(4)	117.2(3)	N(9)-N(10)-Pd(3)	117.1(3)
C(18)-N(5)-Pd(4)	127.0(3)	N(12)-N(11)-C(39)	109.4(3)
C(20)-N(6)-N(5)	108.5(3)	N(12)-N(11)-Pd(4)	117.5(3)
C(20)-N(6)-Pd(5)	128.5(3)	N(5)-N(6)-Pd(5)	118.4(3)

**Table S4.** Selective bond distance (Å) and angle (°) of complex **2b**•10NO<sub>3</sub><sup>-</sup>

Bond	Dist.[Å]	Bond	Dist.[Å]
Pd1-N7	1.983(6)	Pd4-N1	2.017(8)
Pd1-N11	2.003(7)	N8-C31	1.352(11)
Pd1-N12	2.031(7)	Pd4-N2	2.000(7)
N1-C55	1.390(11)	N9-C17	1.357(12)
Pd1-N21	2.014(7)	Pd4-N3	2.012(7)
N2-C54	1.330(12)	N9-C13	1.355(13)
Pd2-N8	2.022(6)	Pd4-N5	2.033(8)
N2-C50	1.344(11)	N10-C18	1.378(13)
Pd2-N9	2.014(8)	Pd5-N13	1.995(8)
N3-N28	1.332(11)	N10-C22	1.347(12)
Pd2-N10	2.009(6)	Pd5-N16	2.027(8)
N3-C62	1.375(12)	N11-C1	1.370(13)
Pd2-N22	2.010(8)	Pd5-N19	2.025(8)
N5-C42	1.336(12)	N11-C5	1.387(11)
Pd3-N14	2.015(6)	Pd5-N20	2.011(8)
N5-N6	1.353(10)	N12-C6	1.341(11)
Pd3-N15	2.011(6)	N12-C10	1.319(13)
N6-C41	1.318(11)	N13-N14	1.377(9)

Pd3-N17	1.985(8)	N13-C46	1.316(13)
N7-C33	1.354(10)	N14-C48	1.319(12)
Pd3-N18	2.006(6)	N15-N16	1.369(9)
N7-N8	1.353(9)	Pd1-N7	1.983(6)
Bond	Angel[°]	Bond	Angel[°]
N7-Pd1-N11	96.1(3)	N14-Pd3-N18	96.8(3)
N16-Pd5-N20	178.3(3)	N5-N6-C41	110.8(7)
N7-Pd1-N12	177.3(3)	N15-Pd3-N17	98.0(3)
N19-Pd5-N20	82.2(3)	Pd1-N7-N8	118.1(5)
N7-Pd1-N21	84.9(3)	N15-Pd3-N18	176.8(3)
Pd4-N1-C55	113.6(5)	Pd1-N7-C33	131.7(6)
		N17-Pd3-N18	79.7(3)
N11-Pd1-N12	81.2(3)	N8-N7-C33	107.7(6)
Pd4-N1-C59	126.8(7)	N1-Pd4-N2	81.0(3)
N11-Pd1-N21	179.0(3)	Pd2-N8-N7	118.4(5)
C55-N1-C59	119.5(8)	N1-Pd4-N3	97.8(3)
N12-Pd1-N21	97.8(3)	Pd2-N8-C31	128.0(5)
Pd4-N2-C50	124.7(6)	N1-Pd4-N5	176.0(3)
N8-Pd2-N9	97.6(3)	N7-N8-C31	110.2(6)
Pd4-N2-C54	115.1(6)	N2-Pd4-N3	178.2(3)
N8-Pd2-N10	178.3(3)	Pd2-N9-C13	127.2(7)
C50-N2-C54	120.3(8)	N2-Pd4-N5	95.3(3)
N8-Pd2-N22	84.4(3)	Pd2-N9-C17	114.2(6)
Pd4-N3-N28	120.7(5)	N3-Pd4-N5	85.9(3)
N9-Pd2-N10	80.8(3)	C13-N9-C17	118.6(8)
Pd4-N3-C62	126.1(6)	N13-Pd5-N16	85.1(3)
N9-Pd2-N22	177.1(3)	Pd2-N10-C18	115.2(6)
N28-N3-C62	105.1(7)	N13-Pd5-N19	177.2(3)
N10-Pd2-N22	97.3(3)	Pd2-N10-C22	125.7(6)
Pd4-N5-N6	120.4(5)	N13-Pd5-N20	95.5(3)
N14-Pd3-N15	85.6(3)	C18-N10 -C22	119.2(7)
Pd4-N5-C42	129.2(6)	N16-Pd5-N19	97.2(3)
N14-Pd3-N17	176.4(3)	Pd1-N11-C1	127.1(6)
N6-N5-C42	108.4(7)		

**Table S5.** Selective bond distance (Å) and angle (°) of complex **3•12PF<sub>6</sub><sup>-</sup>**

Bond	Bond
Dist.[Å]	Dist.[Å]
Pd1-N1	1.984(3)
	Pd4-N18
	2.017(3)

Pd1-N2	2.014(3)	Pd4-N20	2.051(3)
Pd1-N13	1.971(3)	Pd5-N9	2.029(3)
Pd1-N15	2.047(3)	Pd5-N10	1.947(3)
Pd2-N3	2.030(3)	Pd5-N21	1.969(2)
Pd2-N4	2.034(3)	Pd5-N23	1.970(3)
Pd2-N14	1.976(3)	Pd6-N11	2.037(3)
Pd2-N16	2.029(3)	Pd6-N12	2.023(3)
Pd3-N5	2.013(3)	Pd6-N22	1.974(3)
Pd3-N6	2.028(3)	Pd6-N24	1.961(3)
Pd3-N17	1.993(3)		
Pd3-N19	1.993(3)		
Pd4-N7	2.056(3)		
Pd4-N8	1.993(3)		
Bond	Angel[°]	Bond	Angel[°]
N1-Pd1-N2	82.96(11)	N4-Pd2-N16	173.94(12)
N10-Pd5-N23	174.33(11)	N14-Pd2-N16	87.91(11)
N1-Pd1-N13	95.09(12)	N5-Pd3-N6	83.07(11)
N21-Pd5-N23	85.93(11)	N5-Pd3-N17	176.63(10)
N1-Pd1-N15	176.74(11)	N5-Pd3-N19	96.51(11)
N11-Pd6 -N12	81.41(11)	N6-Pd3-N17	93.93(11)
N2-Pd1-N13	176.11(12)	N6-Pd3-N19	176.69(12)
N11-Pd6-N22	93.95(11)	N17-Pd3-N19	86.40(11)
N2-Pd1-N15	95.71(11)	N7-Pd4-N8	84.37(11)
N11-Pd6-N24	177.73(12)	N7-Pd4-N18	89.87(11)
N13-Pd1-N15	86.41(11)	N7-Pd4-N20	173.13(11)
N12-Pd6-N22	175.07(10)	N8-Pd4-N18	173.92(11)
N3-Pd2-N4	81.25(11)	N8-Pd4-N20	98.43(11)
N12-Pd6-N24	98.02(11)	N18-Pd4-N20	87.50(11)
N3-Pd2-N14	176.05(11)	N9-Pd5-N10	84.70(12)
N22-Pd6-N24	86.68(11)	N9-Pd5-N21	174.97(12)
N3-Pd2-N16	95.38(11)	N9-Pd5-N23	89.63(12)
N4-Pd2-N14	95.67(11)	N10-Pd5-N21	99.75(11)

**Table S6.** Selective bond distance (Å) and angle (°) of complex **4b**•10NO<sub>3</sub><sup>-</sup>

Bond		Bond	
Dist.[Å]		Dist.[Å]	
Pd1-N1	1.989(5)	Pd10-N42	2.002(5)
Pd8-N15	1.984(4)	Pd4-N7	1.998(4)
Pd1-N2	1.923(5)	Pd4-N8	2.019(5)
Pd8-N16	2.027(5)	Pd4-N27	2.029(5)
Pd1-N21	2.144(5)	Pd4-N29	1.978(4)
Pd8-N36	1.986(4)		

Pd1-N43	2.009(7)	Pd5-N9	1.987(4)
Pd8-N38	2.050(5)	Pd5-N10	2.036(4)
Pd2-N3	1.996(5)	Pd5-N28	2.042(5)
Pd9-N17	1.969(4)	Pd5-N30	2.015(4)
Pd2-N4	1.994(6)	Pd6-N11	2.030(5)
Pd9-N18	1.991(4)	Pd6-N12	1.994(4)
Pd2-N23	1.960(5)	Pd6-N31	2.028(4)
Pd9-N39	2.004(4)	Pd6-N33	2.024(5)
Pd2-N25	2.024(5)	Pd7-N13	2.002(5)
Pd9-N41	2.036(5)	Pd7-N14	1.985(4)
Pd3-N5	1.992(4)	Pd7-N35	1.999(5)
Pd10-N19	2.043(4)	Pd7-N37	1.975(4)
Pd3-N6	1.985(5)	Pd10-N40	1.981(5)
Pd10-N20	2.006(5)		
Pd3-N24	2.034(5)		
Pd3-N26	2.029(5)		
Bond	Angel[°]	Bond	Angel[°]
N1-Pd1-N2	81.9(2)	N5-Pd3-N26	175.99(19)
N10-Pd5-N30	96.84(18)	N15-Pd8-N16	80.70(18)
N1-Pd1-N21	176.4(2)	N6-Pd3-N24	176.67(19)
N28-Pd5-N30	85.69(18)	N15-Pd8-N36	176.2(2)
N1-Pd1-N43	97.5(2)	N6-Pd3-N26	95.73(19)
N11-Pd6-N12	79.60(18)	N15-Pd8-N38	97.80(18)
N2-Pd1-N21	95.3(2)	N24-Pd3-N26	87.52(19)
N11-Pd6-N31	95.85(18)	N16-Pd8-N36	96.08(18)
N2-Pd1-N43	178.0(2)	N7-Pd4-N8	80.55(18)
N11-Pd6-N33	175.60(16)	N16-Pd8-N38	178.45(18)
N21-Pd1-N43	85.3(2)	N7-Pd4-N27	94.64(19)
N12-Pd6-N31	175.36(19)	N36-Pd8-N38	85.41(18)
N3-Pd2-N4	81.9(2)	N7-Pd4-N29	178.51(19)
N12-Pd6-N33	96.42(18)	N17-Pd9-N18	80.58(18)
N3-Pd2-N23	100.31(19)	N8-Pd4-N27	174.97(17)
N31-Pd6-N33	88.10(18)	N17-Pd9-N39	177.4(2)
N3-Pd2-N25	174.62(19)	N8-Pd4-N29	97.98(18)
N13-Pd7-N14	81.44(19)	N17-Pd9-N41	96.37(19)
N4-Pd2-N23	177.8(2)	N27-Pd4-N29	86.84(18)
N13-Pd7-N35	177.16(17)	N18-Pd9-N39	98.13(17)
N4-Pd2-N25	94.3(2)	N9-Pd5-N10	81.50(18)
N13-Pd7-N37	96.36(19)	N18-Pd9-N41	176.67(18)
N23-Pd2-N25	83.53(19)	N9-Pd5-N28	96.00(18)
N14-Pd7-N35	97.95(18)	N39-Pd9-N41	84.97(18)
N5-Pd3-N6	80.38(19)	N9-Pd5-N30	175.92(18)
N14-Pd7-N37	177.45(19)	N19-Pd10-N20	80.43(18)

N5-Pd3-N24 N35-Pd7-N37	96.36(19) 84.20(18)	N10-Pd5-N28	177.42(18)
---------------------------	------------------------	-------------	------------

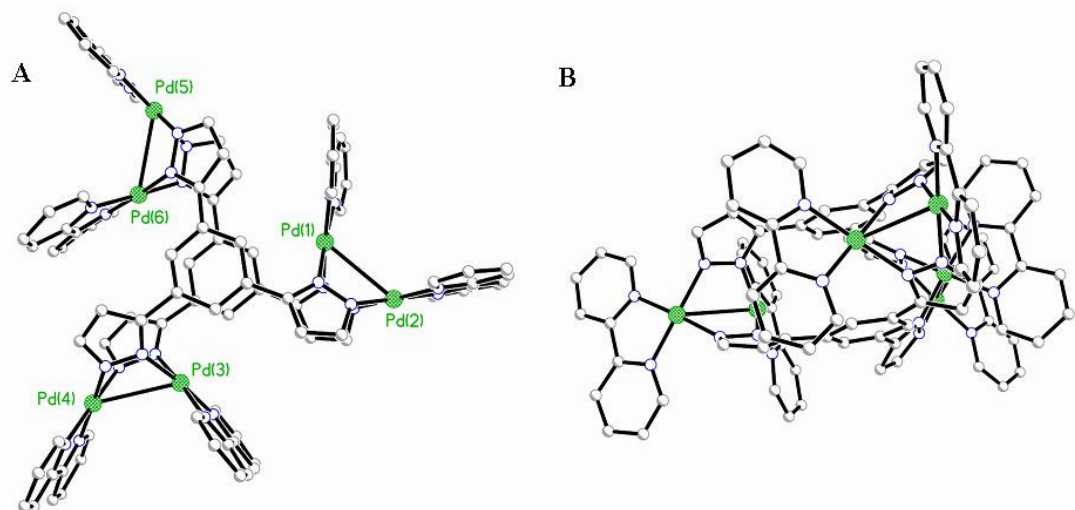


**Figure S28.** The crystal structure of metal-organic cage **1** · 6NO<sub>3</sub><sup>-</sup> ([Pd<sub>6</sub>L<sup>1</sup><sub>2</sub>] · 6 NO<sub>3</sub><sup>-</sup>).

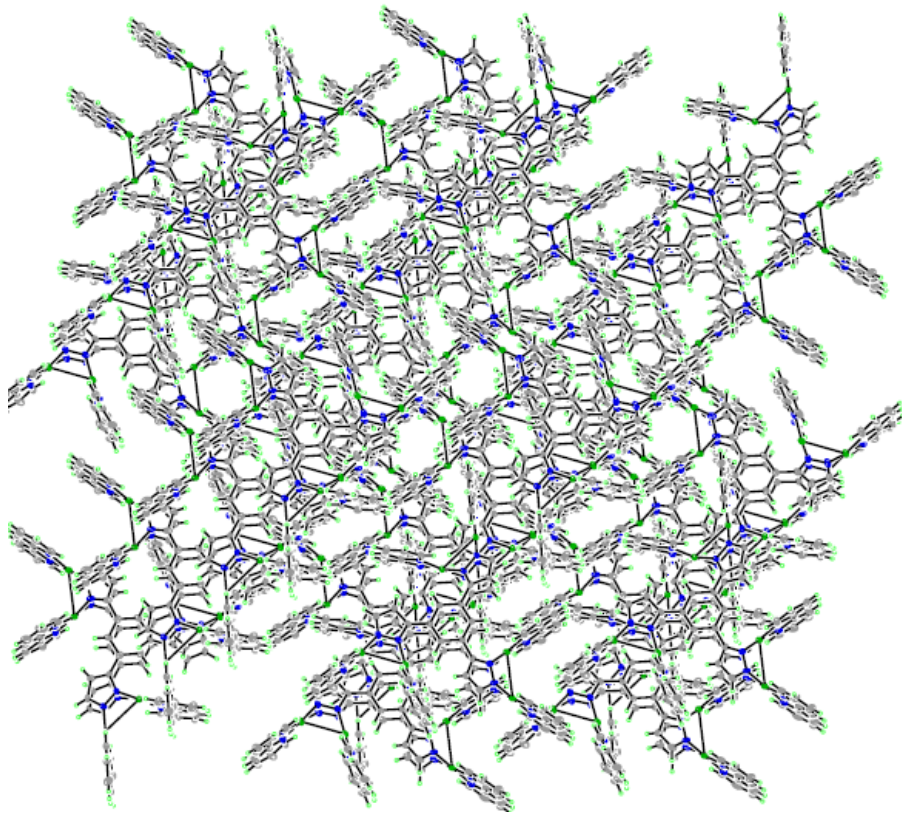


**Figure S29.** Crystal packing of metal-organic cage  $\mathbf{1} \cdot 6\text{NO}_3^-$  ( $[\text{Pd}_6\text{L}^1_2] \cdot 6\text{NO}_3^-$ ) viewed along the c-axis.

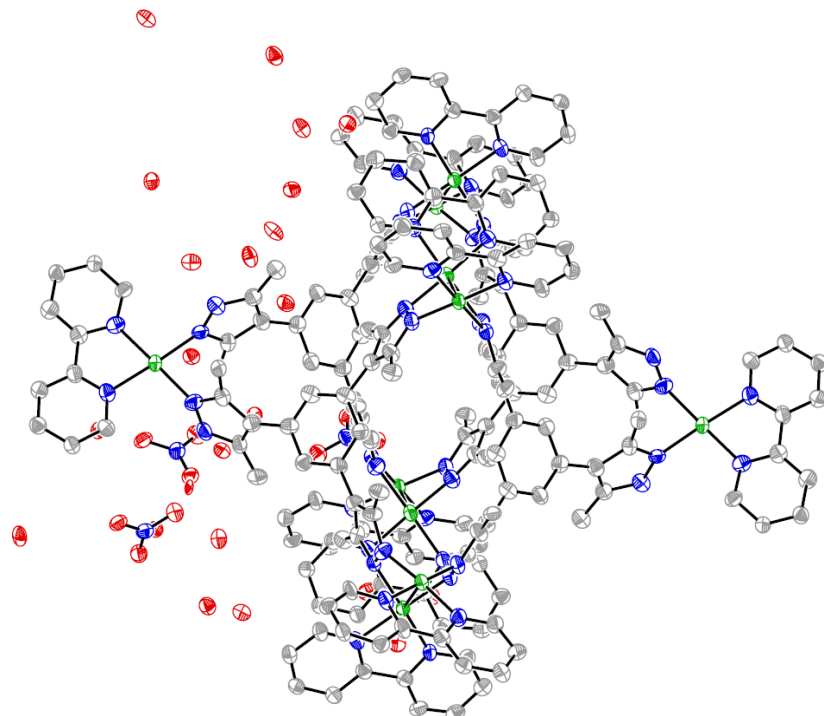


**Figure S30.** The crystal structure of metal-organic cage **2a**·10NO<sub>3</sub><sup>-</sup> ([Pd<sub>10</sub>L<sup>2</sup><sub>4</sub>] · 10NO<sub>3</sub><sup>-</sup>).

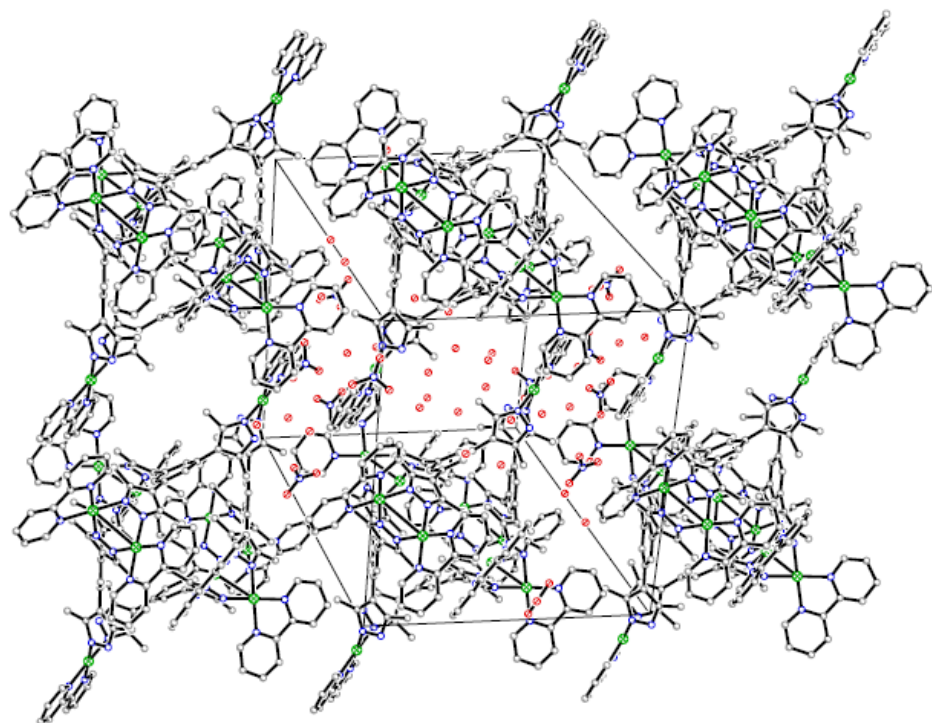


**Figure S31.** Crystal packing of metal-organic cage **2a**·10NO<sub>3</sub><sup>-</sup> ([Pd<sub>10</sub>L<sup>2</sup><sub>4</sub>] · 10NO<sub>3</sub><sup>-</sup>).

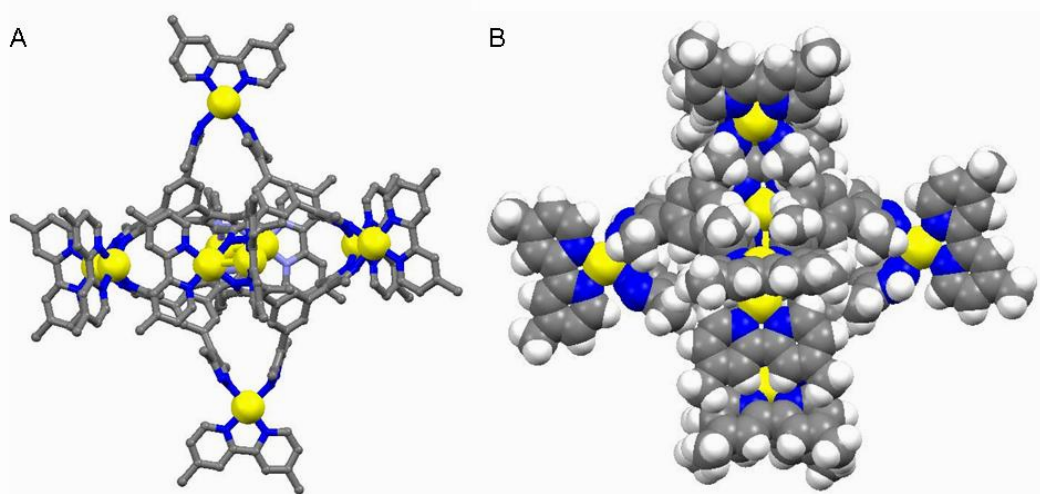


**Figure S32.** The crystal structure of metal-organic cage **2b**·10NO<sub>3</sub><sup>-</sup> ([Pd<sub>10</sub>L<sup>2</sup><sub>4</sub>] · 10NO<sub>3</sub><sup>-</sup>). A, ball and stick model; B, drawn in space-filling mode.

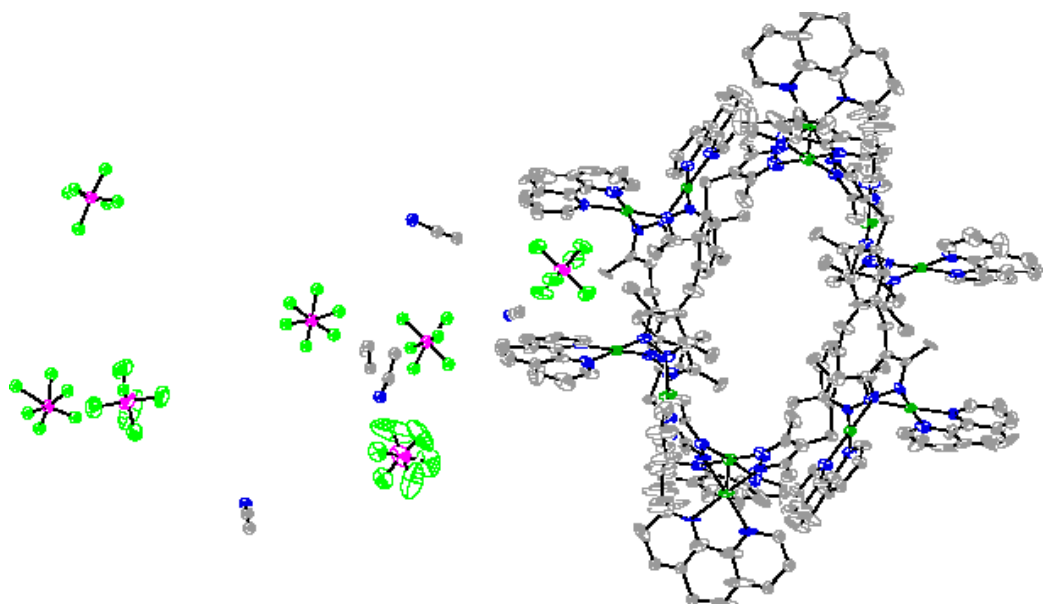


**Figure S33.** The crystal structure of metal-organic cage **3**·12NO<sub>3</sub> ([Pd<sub>12</sub>L<sup>3</sup>]<sup>4-</sup>·12PF<sub>6</sub><sup>-</sup>).

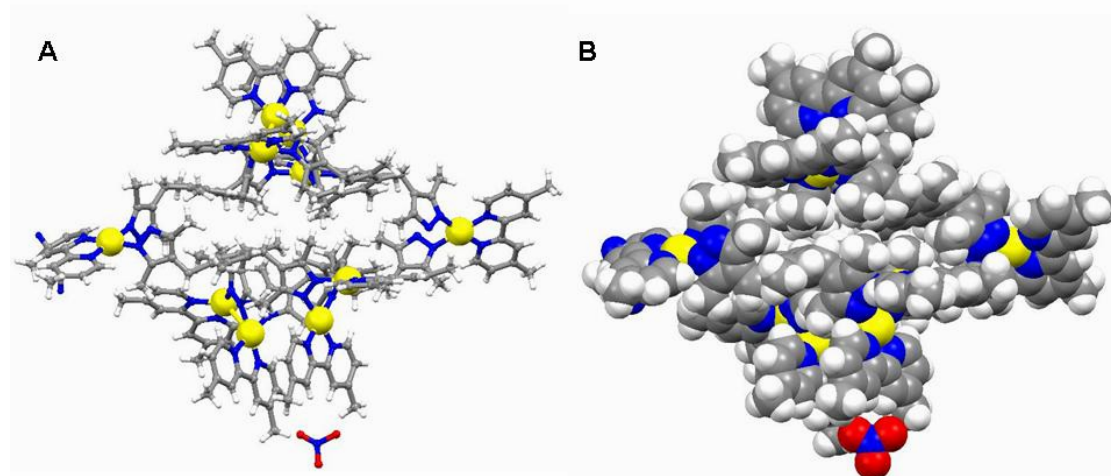


**Figure S34.** The crystal structure of metal-organic cage **4b**·10NO<sub>3</sub><sup>-</sup> ([Pd<sub>10</sub>L<sup>4</sup>]<sup>4-</sup> · 10NO<sub>3</sub><sup>-</sup>). A, ball and stick model; B, drawn in space-filling mode.

#### S4 References

- [1] D. Parker, *Macrocyclic Synthesis- A practical approach*, Oxford, New York, 1996.
- [2] F. Sansonea, S. Barbosa, R. Ungaro. *Eur. J. Org. Chem.* **1998**, 897-902.
- [2] C. D. Gutsche, P. F. Pagoria, *J. Org. Chem.* **1985**, *50*, 5795-5802.
- [3] A. Arduini, M. Fabbi, M. Mantovani, L. Mirone, A. Pochini, A. Secchi, R. Ungaro. *J. Org. Chem.* **1995**, *60*, 1454-1458.